Electrochemical and
Solid-State Letters

Low Temperature Atomic Layer Deposition of Ruthenium Thin Films Using Isopropylmethylbenzene-Cyclohexadiene-Ruthenium and O_2

To cite this article: Tae-Kwang Eom *et al* 2009 *Electrochem. Solid-State Lett.* **12** D85

Electrochemical and Solid-State Letters, **12** (11) D85-D88 (2009)
1099-0062/2009/12(11)/D85/4/$25.00 © The Electrochemical Society

Low Temperature Atomic Layer Deposition of Ruthenium Thin Films Using Isopropylmethylbenzene-Cyclohexadiene-Ruthenium and O_2

Tae-Kwang Eom,[a] Windu Sari,[a] Kyu-Jeong Choi,[b] Woong-Chul Shin,[b] Jae Hyun Kim,[c,*] Do-Joong Lee,[d] Ki-Bum Kim,[d,*] Hyunchul Sohn,[e] and Soo-Hyun Kim[a,*,z]

[a]*School of Materials Science and Engineering, Yeungnam University, Gyeongsangbuk-Do 712-749, Korea*
[b]*NCD Technology, Daejeon 305-764, Korea*
[c]*Division of Nano and BioTechnology, Daegu Gyeongbuk Institute of Science and Technology, Daegu 704-230, Korea*
[d]*Department of Materials Science and Engineering, Seoul National University, Seoul 151-742, Korea*
[e]*Department of Materials Science and Engineering, Yonsei University, Seoul 120-749, Korea*

Ru thin films were deposited by atomic layer deposition (ALD) through alternating exposures of a metallorganic precursor, $C_{16}H_{22}Ru$ [(η6-1-isopropyl-4-methylbenzene) (η4-cyclohexa-1,3-diene)ruthenium(0)] and O_2 at 220°C. The growth rate was 0.1 and 0.086 nm/cycle on TiN and thermally grown SiO_2, respectively. On both substrates, negligible incubation cycles were observed indicating that Ru nucleation was enhanced compared to the results obtained using the cyclopentadienyl-based Ru precursors. Plan-view transmission electron microscopy analysis revealed the formation of a continuous Ru film with a thickness of ~3.5 nm after only 50 ALD cycles. The step coverage was approximately 100% over the contact holes (top opening diameter was 89 nm) with a high aspect ratio (24:1).
 [DOI: 10.1149/1.3207867]

Manuscript submitted June 8, 2009; revised manuscript received July 30, 2009. Published August 20, 2009.

Ru thin films have been widely investigated in semiconductor device technologies, such as an electrode for the capacitor of dynamic random access memory devices,[1] a seed layer for Cu metallization,[2] and a gate material for the metal-oxide-semiconductor transistor,[3] on account of their low resistivity (7.1 μΩ cm), large work function (4.7 eV), and chemical/thermal stability. Ru nanostructures are expected to be used in various systems including nonvolatile memory devices with Ru nanocrystals, the fabrication of nanodevices, and the formation of nanocomposites.[4-8] For these applications, a conformal film deposition technique on a high aspect-ratio trench or hole structure with excellent thickness uniformity and process controllability is essential. In these respects, atomic layer deposition (ALD) can be a potential solution for preparing Ru thin films or nanostructures because ALD uses a self-limiting film growth mode by surface-saturated reactions, which enables atomic-scale control of the film thickness with excellent step coverage.[4]

The results of Ru ALD reported thus far mainly used cyclopendadienyl-based Ru precursors, such as bis(cyclopentadienyl)ruthenium(II) ($RuCp_2$) [9-12] and bis(ethylcyclopentadienyl)ruthenium(II) [$Ru(EtCp)_2$].[5,6,13-15] Both precursors have a metal valence of 2, and metallic Ru films were deposited by oxidative decomposition of the Ru precursor using a suitable reactant, such as O_2. A similar reaction route was also reported using a β-diketonate Ru precursor, such as tris(tetramethyl-heptane-dionate) ruthenium(III) and O_2.[16] However, Ru ALD with these two types of precursors and O_2 has a relatively long incubation time with a lower film growth rate at the initial stages of film deposition, which is related to the delayed nucleation of the film material.[9,11,14-16] This results in a film with a rough morphology, which is unsuitable for conformal film deposition on high aspect-ratio structures. To reduce the incubation time, plasma-enhanced atomic layer deposition (PEALD), which employs NH_3 plasma as a reactant instead of O_2 gas, has been studied.[14,15,17] The Ru film deposited by PEALD showed a linear film growth rate by the number of the ALD cycles, and initial nuclei density was significantly as high as 10^{12} cm^{-2} by transmission electron microscope (TEM) analysis.[14] However, plasma processes usually have limited applications to the film deposition in high aspect-ratio nanostructures due to the longer Debye length and molecular mean free path in the plasma than typical dimension of nanostructures.[18]

It was reported that Ru ALD with an O_2 reactant showed a different incubation time according to the substrates or surface conditions.[6,11,14] Ru film deposited on the HfO_2 surface showed a shorter incubation time than that on the SiO_2 and H-terminated Si substrate. The NH_3 plasma-nitrided SiO_2 surface and SiN_x surface provided considerably more sites for adsorption of the Ru precursor. These aspects suggest that the initial nucleation behavior of an ALD-Ru film differs according to the surface conditions, and the step coverage of a Ru film can be enhanced by modifying the surface to provide more active sites for the Ru precursor. Recently, it was reported that the incubation time for Ru ALD on Si, SiO_2, TiN, and TiO_2 can be reduced using a metallorganic Ru precursor of 2,4-(dimethylpentadienyl)(ethylcyclopentadienyl)Ru(II) with a half-open molecular ligand.[7,19]

This article reports Ru ALD at a low temperature of 220°C using a Ru metallorganic precursor, $C_{16}H_{22}Ru$ [(η6-1-isopropyl-4-methylbenzene) (η4-cyclohexa-1,3-diene)ruthenium], and O_2 on thermally grown SiO_2 and TiN substrates. TEM analysis was performed to measure the film thickness according to the deposition conditions and to examine the nucleation and growth behavior of ALD-Ru. This study also investigated the step coverage at the high aspect-ratio (~24:1) contact hole structure and a possible interfacial layer between Ru and TiN by high resolution transmission electron microscopy (HRTEM) for applications of ALD-Ru to capacitor electrodes and seed layers for Cu metallization.

Ru films were deposited using a 4 in. diameter wafer-scale traveling wave-type ALD reactor (NCD Technology, Lucida D100) at 220°C and 1 Torr using a Ru precursor, $C_{16}H_{22}Ru$ (DNF Co.). The Ru precursor was prepared as follows. A solution of ruthenium trichloride hydrate in ethanol was treated with α-terpinene and refluxed for 5 h. The orange-yellow microcrystalline product di-μ-chloro-bis[chloro(η^6-1-isopropyl-4-methylbenzene)ruthenium(II)] was collected in a glass funnel, washed with hexane, and dried in vacuo. Then, a solution of the above product and Na_2CO_3 in a mixture of ethanol and freshly distilled 1,3-cyclohexadiene was refluxed for 4.5 h. Finally, after evaporation of the solvents and vacuum distillation, a yellow product of (η6-1-isopropyl-4-methylbenzene) (η4-cyclohexa-1,3-diene)ruthenium(0) was obtained. Figure 1 shows the molecular structure of the Ru precursor used in this study.

* Electrochemical Society Active Member.
z E-mail: soohyun@ynu.ac.kr

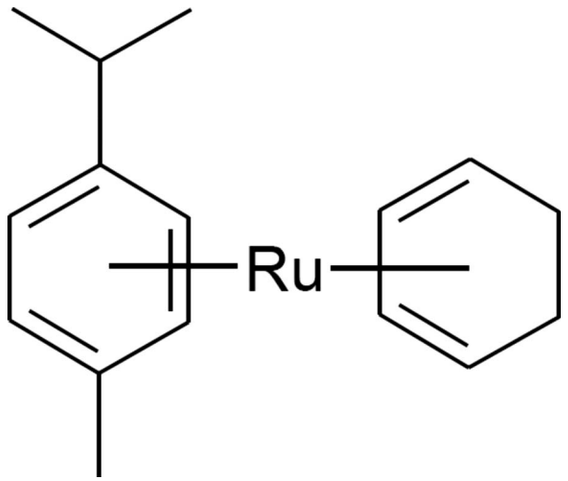

Figure 1. The molecular structure of the Ru precursor used in this study.

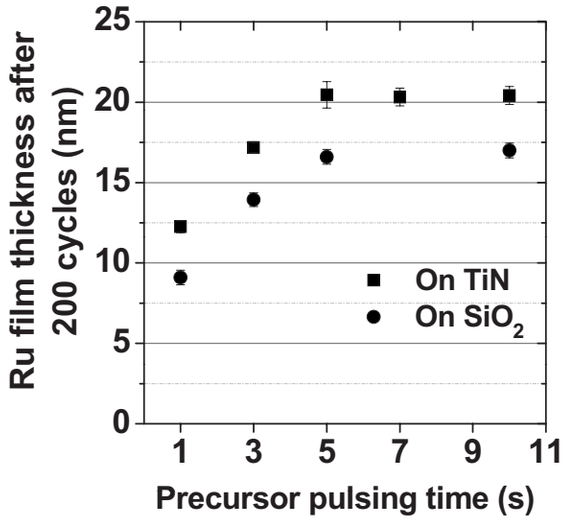

Figure 2. Ru film thickness deposited on TiN (square symbol) and thermally grown SiO_2 (circle symbol) substrates after 200 ALD cycles as a function of the Ru precursor pulsing time. The thicknesses were measured by XTEM.

It is a liquid compound with a high vapor pressure of 1 Torr at 134°C, the metal valence in the precursor is 0, and it is expected that this provides enhanced nucleation of Ru on thermally grown SiO_2 and TiN substrates. Ru precursor vapor was generated in a bubbler at 100°C and carried into the process chamber by N_2 (99.999%) at a flow rate of 10 sccm. The line temperature for precursor delivery was kept at 130°C to prevent condensation of the precursor. The reactant was O_2 at a flow rate of 30 sccm (FC-280SA Tylan mass flow controller). One ALD cycle consisted of a Ru precursor pulse, purging, O_2 pulse, and purging. The precursor pulsing time was varied from 1 to 10 s to determine the conditions for the self-limiting film growth of Ru. The typical purging time (N_2) after Ru precursor was long (10 s) enough to confirm that the growth rate was saturated at this purging time. The oxygen pulsing time was fixed to 0.1 s. The valves used in this study (KITZ high temperature valve, KD4CS-VFM-EP) guarantee the control of 36 ms for valve switching. The ALD-Ru thin films were grown on the chemical-vapor-deposited TiN and thermally grown SiO_2.

Because of the very thin ALD-Ru films in this study 3–20 nm, cross-sectional view transmission electron microscopy (XTEM, Technai F20 equipped with 200 kV accelerating voltage and field-emission gun) was used to measure the film thickness accurately. XTEM was also used to characterize the microstructure of the Ru film and a possible interfacial layer formed on TiN during Ru deposition. The resistivity of the ALD-Ru film was determined by considering the sheet resistances measured using a four-point probe and the film thicknesses. X-ray diffraction using Cu Kα radiation ($\lambda = 1.5406$ Å) at the power of 1.5 kW and electron diffraction analysis were performed for phase identification. Plan-view TEM analysis was used to clearly observe the nucleation behavior of Ru on SiO_2. Finally, the step coverage was examined at the contact hole with an aspect ratio of ~24 (the height was ~2.15 μm, the top opening diameter was 89 nm, and the bottom diameter was ~80 nm).

The self-limiting growth behavior, which is the key characteristics of ALD, was examined at a deposition temperature of 220°C. The dependence of Ru growth on the precursor pulsing time was examined by measuring the film thickness after 200 reaction cycles. Figure 2 shows the film thicknesses of the ALD-Ru films with different precursor pulsing times on the thermally grown SiO_2 and TiN. On both substrates, the film thickness after 200 reaction cycles became saturated at a precursor pulsing time longer than 5 s. This suggests that no thermal self-decomposition of the precursor occurs at this temperature, and deposition is accomplished by a surface reaction between the adsorbed precursors and reactants. However, at all precursor pulsing times, the thickness was greater on the TiN substrate than on the thermally grown SiO_2 substrate, indicating that the TiN surface provides more favorable sites for Ru precursor adsorption.

Figure 3 shows the film thickness as a function of the number of reaction cycles at 220°C. In Fig. 3, the pulsing times for the Ru precursors and O_2 reactant to accomplish a saturation reaction were 5 and 0.1 s, respectively. The film thickness increased linearly with an increasing number of reaction cycles at the thickness range of 2–20 nm. Therefore, the film thickness can be adjusted easily and accurately by the number of reaction cycles. The growth rates on the TiN and SiO_2 substrates determined by linear fitting were 0.1 and 0.086 nm/cycle, respectively. The incubation time, which was estimated by the intercept of Fig. 3 with the abscissa at the origin, was almost zero on the TiN and very short (~11 cycles) on the SiO_2

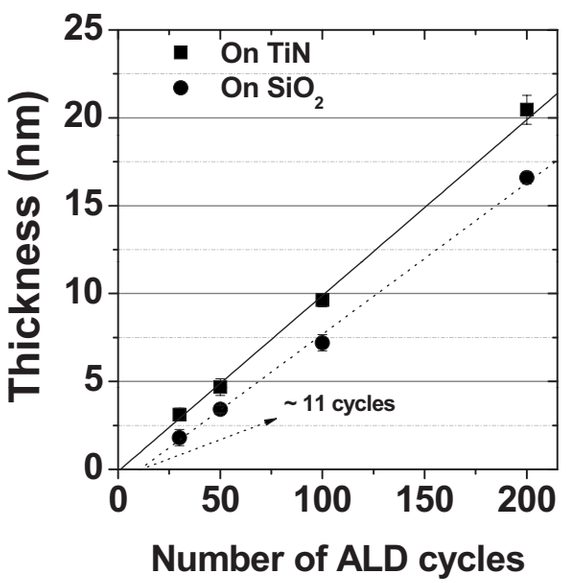

Figure 3. Ru film thickness as a function of the number of reaction cycles. The squares and circles represent the thickness of the film deposited on TiN and thermally grown SiO_2, respectively. The lines indicate the linearly fitted line for the thickness data.

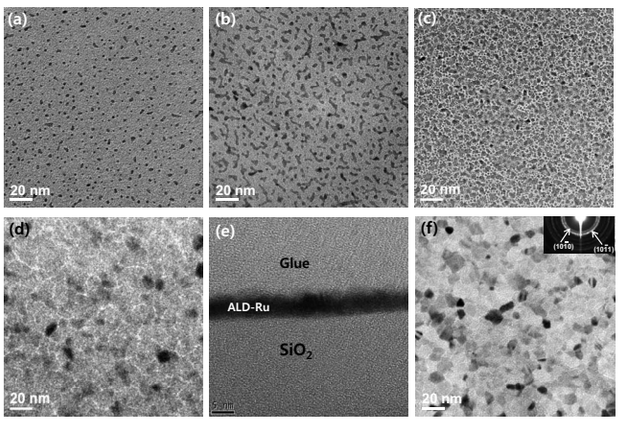

Figure 4. TEM analysis of Ru deposited on a thermally grown SiO_2 substrate. Plan-view TEM image after (a) 7, (b) 10, (c) 30, and (d) 50 ALD cycles. (e) XTEM image of ALD after 50 ALD cycles. (f) Plan-view TEM image after 100 ALD cycles.

substrate, indicating rapid nucleation of the Ru films on both surfaces. This is a different behavior from that observed with the Ru ALD films deposited using $RuCp_2$ [9,11] or $Ru(EtCp)_2$ [14,15,17] and O_2, where rather long incubation times were observed on thermally grown SiO_2, H-terminated Si, ALD-Al_2O_3, ALD-TiO_2, ALD-Ta_2O_5, and TiN substrates. Because a shorter incubation time indicates a higher nucleation rate, it is clear that the precursor used in this study leads to a higher nucleation rate than the Cp-based Ru(II) precursors.

Figure 4 shows the morphology of the ALD-Ru films on a thermally grown SiO_2 substrate with the number of ALD cycles, as characterized by TEM analysis. The Ru nuclei were clearly visible after only three ALD cycles (not shown here). As the ALD cycles increased, the nuclei density also increased and the maximum density of the Ru nuclei was 2.1×10^{12} cm^{-2} on SiO_2 at seven ALD cycles (Fig. 4a). At 10 ALD cycles, coalescence of Ru nuclei occurred at some regions of the SiO_2 surface (Fig. 4b). As the number of ALD cycles was increased to 30 (Fig. 4c), the aggregation and coalescence of Ru nuclei occurs on most of the SiO_2 surface. After 50 ALD cycles (Fig. 4d), a continuous Ru film with a thickness of ~3.5 nm (Fig. 4e) was formed. At 100 ALD cycles (Fig. 4f), a well-developed crystalline Ru film was formed. The corresponding selected area electron diffraction pattern (the inset of Fig. 4f) clearly shows that the film forms Ru with a hexagonal closed-packed structure (a = 2.705 Å and c = 4.281 Å), not RuO_2 with a rutile structure. The resistivity of the ~16.2 nm thick Ru film was determined to be ~36 μΩ cm, indicating that a metallic Ru film had formed. A metallic Ru–Ru bond was also from X-ray photoelectron spectroscopy analysis and only ~4 atom % of oxygen was detected in the ALD-Ru film (not shown here).

These results were compared with those from the liquid precursor of $Ru(II)(EtCp)_2$ precursor. Yim et al.[14] reported that the ALD-Ru film deposited at 300°C was not continuous on thermally grown SiO_2 even after 500 ALD cycles using the $Ru(EtCp)_2$ precursor and O_2 reactant, and the calculated incubation time from the fitting of the thickness with the number of ALD cycles (such as Fig. 3) was as high as ~210, and still as high as ~50 cycles on the TiN substrate.[17] The maximum density of Ru nuclei on SiO_2 was only 5.7×10^{10} cm^{-2} on SiO_2 at 500 ALD cycles.[14] Although they could improve nucleation on the SiO_2 surface by NH_3 plasma pretreatment, a continuous Ru film was not formed after 110 ALD cycles. Therefore, these results clearly show that the nucleation of ALD-Ru on SiO_2 is significantly improved using the Ru precursor and that a continuous ALD-Ru film forms much faster than that using the $Ru(EtCp)_2$ precursor. This is very important considering that poor nucleation on a dielectric surface is the main bottleneck for the implementation of ALD-Ru to the continuously shrinking semiconductor devices.

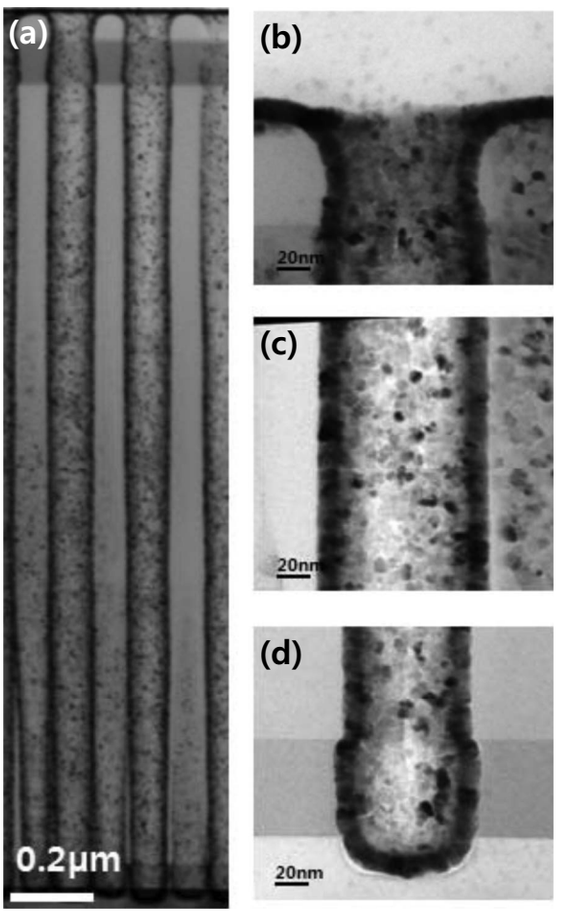

Figure 5. (a) XTEM image of the contact hole structure (aspect ratio is ~24, top diameter is ~89 nm, and bottom diameter is ~80 nm) with the Ru layer. The magnified image at the (b) top of the contact, (c) middle of the contact, and (d) bottom of the contact.

This study also examined the step coverage of an ALD-Ru film deposited on a hole-type capacitor contact with an aspect ratio of ~24, a top opening diameter of 89 nm, and a bottom diameter of 80 nm formed in the SiO_2 layer. Figure 5a shows an XTEM image of the overall contact with the ALD-Ru layer grown under the following growth conditions: Deposition temperature is 220°C, precursor pulsing time is 5 s, O_2 pulsing time is 0.1 s, and purging time is 10 s. The magnified images at the top (Fig. 5b), middle (Fig. 5c), and bottom (Fig. 5d) of the contact showed ALD-Ru thicknesses of 11.9, 11.9, and 11.3 nm, respectively. This gives a 95% step coverage (defined by the bottom thickness/top thickness). To the best of the author's knowledge, this is the best value ever reported considering both the aspect ratio and the contact diameter. The excellent step coverage also shows that our Ru film was deposited under ideal ALD growth conditions without partial decomposition of the precursor.[20]

Finally, we examined the formation of an interfacial oxide layer, which might have formed on the TiN surface during Ru deposition because ALD-Ru has potential applications as a seed layer for the Cu electroplating process of advanced semiconductor devices. Here, the seed layer is typically deposited on a diffusion barrier, such as TiN, TaN, and WN_x. Figure 6 shows a cross-sectional view HRTEM image of an ALD-Ru film deposited on TiN. Lattice fringes indicating the formation of crystalline Ru were clearly shown. There was

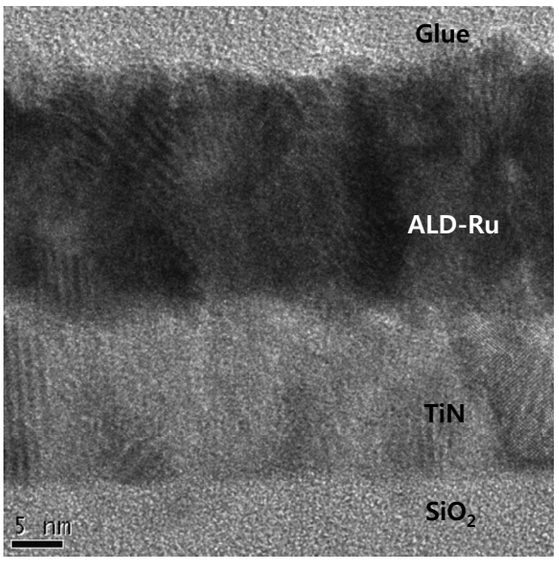

Figure 6. Cross-sectional view HRTEM image of a Ru film deposited on TiN.

no interfacial oxide between the Ru and TiN, such as TiO_x, even though O_2 was used as a reactant. Previously, it was reported that TiO_2 was formed on TiN during the high temperature oxidation of TiN films.[21-23] Although data on TiN oxidation at 220°C are unavailable, Tompkins[22] showed that the oxidation of TiN is very slow at 350°C and its kinetics is even slower in a dry O_2 environment compared to a room air environment. It was also reported that an initiation time of 338 min is required for the oxidation of TiN. This suggests negligible oxidation of the TiN surface during Ru ALD at 220°C. These results also showed that the incubation time was almost zero during Ru ALD on the TiN surface (Fig. 3), indicating that a continuous Ru film could be formed after a few ALD cycles. Therefore, the growing Ru film can protect the TiN surface from oxidation by the O_2 reactant supply. This consideration shows that the current ALD-Ru process can also be applied to the deposition of a seed layer for Cu metallization.

In summary, this study investigated the Ru ALD using a Ru metallorganic precursor, $C_{16}H_{22}Ru$, and O_2 reactant at 220°C. The typical ALD characteristics, such as self-limited film growth and linear dependency of the film growth rate on the number of ALD cycles, were confirmed from thickness measurements using XTEM. The growth rates on TiN and thermally grown SiO_2 were 0.1 and 0.086 nm/cycle, respectively. These results clearly show that Ru nucleation is greatly enhanced compared to the results using typical Cp-based Ru(II) metallorganic precursors. No interfacial oxide was formed between Ru and TiN during ALD-Ru deposition, even though the O_2 reactant was used, which might be due to the low deposition temperature and negligible incubation time. Overall, the current Ru ALD process can be integrated successfully into the deposition of the seed layer for Cu metallization as well as the electrode of capacitors or gate electrodes in continuously shrinking semiconductor devices.

Acknowledgments

This research was supported by the Yeungnam University research grants in 2008. We thank Dr. Zin-Mook Yim in DNF Co., Korea, for providing the Ru precursor.

Yeungnam University assisted in meeting the publication costs of this article.

References

1. S. K. Kim, W.-D. Kim, K.-M. Kim, C. S. Hwang, and J. Jeong, *Appl. Phys. Lett.*, **85**, 4112 (2004).
2. M. W. Lane, C. E. Murray, F. R. McFeely, P. M. Vereecken, and R. Rosenberg, *Appl. Phys. Lett.*, **83**, 2330 (2003).
3. Y.-S. Suh, H. Lazar, B. Chen, J.-H. Lee, and V. Misraa, *J. Electrochem. Soc.*, **152**, F138 (2005).
4. H. Kim, H.-B.-R. Lee, and W.-J. Maeng, *Thin Solid Films*, **517**, 2563 (2009).
5. S.-S. Yim, M.-S. Lee, K.-S. Kim, and K.-B. Kim, *Appl. Phys. Lett.*, **89**, 093115 (2006).
6. D.-J. Lee, S.-S. Yim, K.-S. Kim, S.-H. Kim, and K.-B. Kim, *Electrochem. Solid-State Lett.*, **11**, K61 (2008).
7. W.-H. Kim, S.-J. Park, J.-Y. Son, and H. Kim, *Nanotechnology*, **19**, 045302 (2008).
8. J. Biener, T. F. Baumann, Y. Wang, E. J. Nelson, S. O. Kucheyev, A. V. Hamza, M. Kemell, M. Ritala. and M. Leskelä, *Nanotechnology*, **18**, 055303 (2007).
9. T. Aaltonen, P. Alën, M. Ritala, and M. Leskelä, *Chem. Vap. Deposition*, **9**, 45 (2003).
10. T. Aaltonen, A. Rahtu, M. Ritala, and M. Leskelä, *Electrochem. Solid-State Lett.*, **6**, C130 (2003).
11. K. J. Park, D. B. Terry, M. Stewart, and G. N. Parsons, *Langmuir*, **23**, 6106 (2007).
12. S.-J. Park, W.-H. Kim, W.-J. Maeng, Y. S. Yang, C. G. Park, H. Kim, K.-N. Lee, S.-W. Jung, and W. K. Seong, *Thin Solid Films*, **516**, 7345 (2008).
13. O.-K. Kwon, J.-H. Kim, H.-S. Park, and S.-W. Kang, *J. Electrochem. Soc.*, **151**, G109 (2004).
14. S.-S. Yim, D.-J. Lee, K.-S. Kim, S.-H. Kim, T.-S. Yoon, and K.-B. Kim, *J. Appl. Phys.*, **103**, 113509 (2008).
15. S.-J. Park, W.-H. Kim, H.-B.-R. Lee, W. J. Maeng, and H. Kim, *Microelectron. Eng.*, **85**, 39 (2008).
16. T. Aaltonen, P. Alën, M. Ritala, and M. Leskelä, *Chem. Vap. Deposition*, **10**, 215 (2004).
17. O.-K. Kwon, S.-H. Kwon, H.-S. Park, and S.-W. Kang, *J. Electrochem. Soc.*, **151**, C753 (2004).
18. Y.-B. Jiang, N. Liu, H. Gerung, J. L. Cecchi, and C. Jeffrey Brinker, *J. Am. Chem. Soc.*, **128**, 11018 (2006).
19. S.-K. Kim, S. Y. Lee, S. W. Lee, G. W. Hwang, C. S. Hwang, J. W. Lee, and J. Jeong, *J. Electrochem. Soc.*, **154**, D95 (2007).
20. R. G. Gordon, D. Hausmann, E. Kim, and H. Shepard, *Chem. Vap. Deposition*, **9**, 73 (2003).
21. I. Suni, D. Sigurd, K. T. Ho, and M.-A. Nicolet, *J. Electrochem. Soc.*, **130**, 1210 (1983).
22. H. G. Tompkins, *J. Appl. Phys.*, **70**, 3876 (1991).
23. P. C. McIntyre, S. R. Summerfelt, and C. H. Maggiore, *Appl. Phys. Lett.*, **70**, 711 (1997).